Smart Structures and Systems, Vol. 11, No. 3 (2013) 283-297
DOI: http://dx.doi.org/10.12989/sss.2013.11.3.283

Design and testing of a minimally invasive intervertebral cage for spinal fusion surgery

Walter Anderson*, Cory Chapman, Zohreh Karbaschi, Mohammad Elahinia and Vijay Goel

Mechnical, Industrial and Manufacturing Engineering, University of Toledo, College of Engineering, Toledo 43606, USA

(Received August 3, 2012, Revised October 1, 2012, Accepted October 16, 2012)

Abstract. An innovative cage for spinal fusion surgery is presented within this work. The cage utilizes shape memory alloy for its hinge actuation. Because of the use of SMA, a smaller incision is needed which makes the cage deployment minimally invasive. In the development of the cage, a model for predicting the torsional behavior of SMAs was developed and verified experimentally. The prototype design of the cage was developed and manufactured. The prototype was subjected to static tests per ASTM specifications. The cage survived all of the tests, alluding to its safety within the body.

Keywords: shape memory alloy; spinal fusion; superelastic; intervertebral cage

1. Introduction

Low back pain is a condition that 15 to 20 percent of the US population suffers from (Bigos *et al*. 1994). In some cases, spinal fusion surgery is needed to alleviate pressure on the nerves in the lower back. Currently, placement of spinal fusion cages requires extreme surgeries and cause great deal of trauma. By employing a shape memory alloy (SMA) actuator, an innovative cage design has been developed. The cage's insertion method is minimally invasive and through the use of SMA, the cage is assembling. A CAD model of the cage can be seen in Figs. 1 and 2. Fig. 1 shows the cage after deployment (inside the body). The pyramidal serrations allow for solid fixation without being directionally cumbersome. Fig. 2 shows the cage pre- deployment, or outside the body. As can be seen, the cage forms a straight line and therefore a smaller incision is needed for placement. The different spinal fusion procedures as well as recent attempts at minimally invasive spinal fusion procedures will be reviewed. Following, shape memory alloys used in a torsional medical application and as a torsional actuator will be reviewed.

There are multiple types of spinal fusion surgery including Anterior Lumbar Intervertebral Fusion (ALIF), Posterior Lumbar Intervertebral Fusion (PLIF), Transforaminal Lumbar Intervertebral Fusion (TLIF), eXtreme lateral Lumbar Intervertebral Fusion (XLIF) and Axial Lumbar Intervertebral Fusion (AXLIF). Additionally, multiple cage designs are available for fusion surgeries. A schematic showing the different directions of approach is shown in Fig. 3.

*Corresponding author, E-mail: Walter.B.Anderson@gmail.com

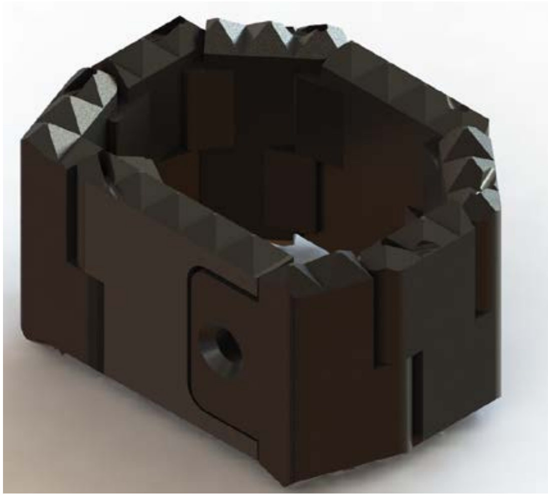

Fig. 1 CAD model of the prototype design after closure inside the body

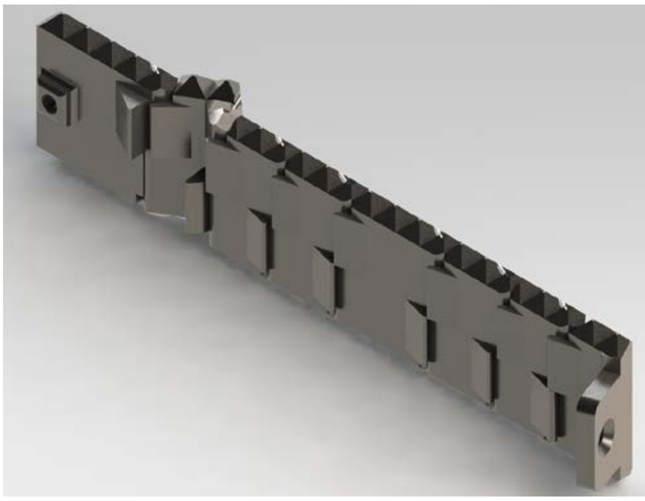

Fig. 2 CAD model of the prototype design, pre-deployment outside the body; the cage forms a line and therefore can be inserted through a small incision

The invasiveness, surgery time and stability can be different depending on which approach is taken. Other existing conditions can affect which approach is taken as well. A general schematic of a spinal fusion operation is shown in Fig. 4. As can be seen, aside from the fusion device itself, there are other implant devices to ensure stability, i.e., pedicle screws. In most fusion surgeries natural or synthetic material is used to encourage bone formation toward fusion of the two vertebral bodies.

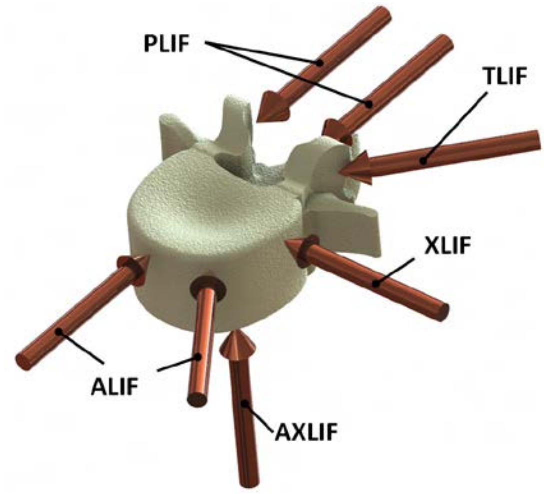

Fig. 3 Different angles of approach for spinal fusion surgery

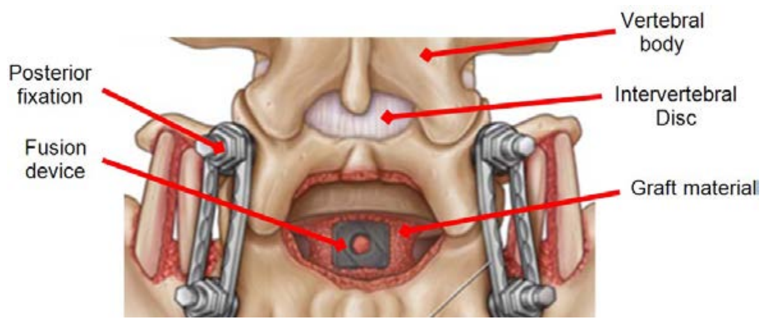

Fig. 4 Nomenclature for posterior fusion (Lipson 2004)

A posterior (PLIF) approach was targeted for this prototype and therefore more emphasis will be put on posterior spinal fusion devices for review. It should be noted that each of the procedures has a unique set of advantages and disadvantages. For PLIF, the incision is made directly at the site of surgery and allows for direct decompression of affected nerves (Burkus 2003). This procedure also allows for direct placement of the implant at the center of rotation and load. The PLIF approach is quite invasive though, as often times multiple boney structures must be removed for cage placement. The prototype cage lessens this detrimental effect due to the small footprint pre-deployment. It should also be noted that PLIF or TLIF are the preferred approaches for physically active patients due to the increased stability that is able to be achieved with this procedure (Brennan and Lauryssen 2000).

The ALIF procedure's advantages lie in the approach. The advantages of anterior placement are less blood loss, less removal of boney structures, no direct nerve exposure, and a shorter procedure time (Burkus 2003, Mayer 1999). However, the vascular structure (abdominal aorta and inferior vena cava) of the spine limits the lumbar vertebrae that can be fused through the ALIF procedure. To be minimally invasive, this procedure must be performed laparoscopically, which requires the surgeon to have considerable skill.

The XLIF procedure is characterized by direct visualization of the cage insertion site and a shorter procedure time than its ALIF counterpart. However, this procedure causes a large amount of trauma to the muscle structures that surround the fusion site. This can be detrimental because these muscular structures help provide stability to the spinal column and can lessen the low back pain experienced by the patient. Furthermore this is a relatively new procedure (Ozgur 2006).

The AXLIF procedure is another newer procedure. AXLIF is limited to the extreme low back (L5-S1 fusion) and is not nearly as versatile as the other procedures. The approach is the primary advantage of AXLIF. Each of the approaches can have a 'minimally invasive' aspect to them.

In an attempt to achieve another type of minimally invasive fusion surgery, Boden *et al*. performed intertransverse process fusion on rabbits and rhesus monkeys (Boden *et al*. 1996). This procedure is fusion of the transverse processes by bone graft placed in between adjacent spinal segments. They further enhanced the surgery by testing the advantages of video assistantship. They showed good results and proved that the video assisted approach is less traumatic to the musculature and the procedure can result in spinal fusion.

Regan *et al*. investigated the advantages of a laparoscopic (transperitoneal approach) and an open anterior approach with BAK (Sulzer SpineTech, Minneapolis, MN) cages (Regan *et al*. 1999). It was found that the laparoscopic group had shorter hospital stays and comparable complications. However, there is a learning curve associated with laparoscopic procedures, but once mastered, it is just as safe and effective.

Shape memory alloys (SMAs) have the potential to bring innovative minimally invasive approaches to multiple medical procedures. Historically, SMA has been a subject for research in multiple fields such as robotics, aerospace and automotive. However, due to the biocompatibility and unique properties, SMAs use in the medical field has expanded. Current medical applications using SMA are stents, bone staples, orthodontic wires, guide wires, filters and steerable catheters (Stoeckel 2002, Duerig *et al*. 1999, Russell 2009, Cragg *et al*. 1983).

Nevertheless, one of the only examples of a medical device that uses nitinol in torsion is the root canal file. Root canal files need to be flexible yet stiff to avoid complications from the surgery and/or to avoid adversely altering the procedure (Walia *et al*. 1988). Nitinol was found to be beneficial over stainless steel with respect to these parameters.

Applications of nitinol used as a torsional actuator is primarily found in the aerospace field. This is primarily due to the advantages of a variable geometry wing as well as the benefits of changing wing camber mid-flight. Icardi and Ferrero performed exploratory research into an adaptive wing using nitinol torsion tubes for camber adjustment and nitinol elements for wing surface manipulation. (Icardi and Ferrero 2009).

Jacob et al. used nitinol torsion camber actuators for development of an inflatable wing unmanned aerial vehicle (UAV) (Jacob *et al*. 2005). They studied the wing design in a FE framework. After the numerical analysis, the authors designed and built an inflatable wing UAV and performed low altitude flight tests.

In one of the few non-aerospace applications, Brook studied the use of an SMA tube as a boom latch release mechanism for satellite deployment (Brook 1983). The author used a 15 W heating element in a SMA tube and achieved 6.78 Joules of work. Brook was able to show the viability of such a mechanism where electrical power is limited. Other researchers have also used nitinol wires to induce torsion. Xiong et al. studied such a system as a general purpose torsional actuator (Xiong *et al*. 2000). They developed a model in an attempt to predict the response of the system but do not compare their numerical results to the experimental findings.

The innovation of prototype cage is realized through the use of shape memory alloy as hinge actuators to drive the invention to a minimally invasive one. With the prototype, a smaller incision (in the annulus and dermal level) and removal of less boney stabilizing structures is possible. Current cage designs require an incision that is at least the same size as the cage; as well as removal of boney structures to make way for cage placement. This directly indicates that the cage will lead to more successful surgeries.

2. Innovative cage design

The intervertebral cage discussed here is a novel approach to spinal fusion surgery. The cage uses SMA hinges to allow for the self-closing design. The main material for the cage is Ti6AlV4 [short: Ti64] which was selected for its biocompatiblity and material properties. The hinges of the cage are nitinol, which is also biocompatible. Both materials also demonstrate excellent fatigue strength.

Ti64 is softer than 316L stainless steel and Cobalt Chromium leading to less stress shielding. This is important in spinal implants because the cortical bone shell can be very thin, leading to the need for revision surgery and other complications. Stress-shielding in when the bone density decreases due to the presence of a stiffer material. In other words, the load sharing is adversely affected. This is extremely problematic in spinal implants because the device can pierce the cortical bone shell ‘sinking’ into one or both vertebrae. This is considered implant failure. As can be seen in Fig. 5, the materials chosen here more closely match those of bone.

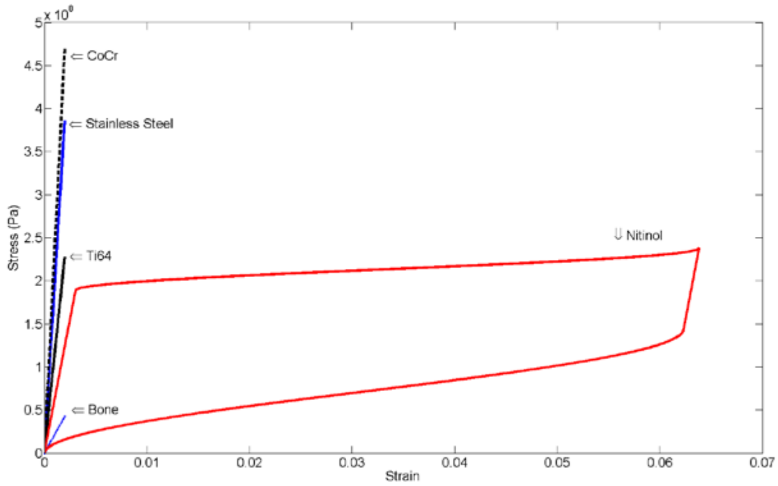

Fig. 5 Comparison of the material response of implant materials and bone

Nitinol was chosen as the hinge material due to its ability to recover large deformations. Here, superelastic nitinol is utilized. For Superelasticity the critical transition temperature (austenite finish, A_f) is below room temperature. This allows for the cage to be straightened before inserting and a drastically smaller and less invasive surgery is needed to be performed.

As aforementioned, the two materials used in the cage are completely biocompatible. Ti64 is generally accepted as a biocompatible material (Kodama 1989), so the focus here will be on the biocompatibility of nitinol.

Ryhanen et al. compared the biocompatibility of nitinol with stainless steel and Ti64 for muscle and perineural tissue (Ryhanen *et al*. 1998). They found no qualitative differences between the materials. Furthermore, they found that nitinol has good in vivo biocompatibility. Kapanen *et al.* studied the effect of nitinol on bone formation (Kapanen *et al*. 2001). They used a rat model to show that nitinol showed no detrimental effects on bone formation. They were able to also determine that nitinol has good biocompatibility. Wever *et al*. determined that nitinol exhibits no cytotoxicity, no adverse sensitization effects, nor any genotoxicity when compared to 316L stainless steel (Wever *et al*. 1997). The authors state (as have many others) that nitinol does not release Ni ions into the corpus system due to the passive Ti02 layer on the outside of the sample.

Assad *et al*. studied the effect of a porous nitinol cage in a sheep model (Assad *et al*. 2003). The authors compared the nitinol cages to a commercially available Ti64 cage (the BAK cage). The sheep were euthanized at 3, 6 and 12 months post-operation and the surrounding tissue was examined. The authors found no statistically significant increase in blood nickel content, immediately or long-term. They further examined the surfaces of the cages using a scanning electron microscope and found no localized pitting or corrosion.

Rhalmi et al. studied nitinol cage failure (as a possible worst case). The authors wanted to study the effect of metallic particle migration into the dura mater for a rabbit model (Rhalmi *et al*. 2007). The authors mechanically fractured porous nitinol cages and implanted the particles. For a comparison study and a control group, some rabbits had Ti64 particles implanted and some underwent surgery without any implant. No cytotoxicity or necrosis of the dura mater was observed in any of the specimens 52 weeks post-operation.

2.1 Hinge design

The SMA hinge design was developed such that the cage would be able to provide enough torque to close within the intervertebral space. The torque angle profile for the wire is shown in Fig. 6. A zoom of the specified design region is shown in Fig. 7. This region of the stress- strain curve was selected such that the cage exhibited near constant torque throughout the actuation cycle. The wire is designed such that it is shape set into a ‘C’ and is forced to assume the position of a ‘Z’, shown in Fig. 8. Using this shape set hinge, a torsional actuator is implemented into the cage causing it to go from the straightened condition (pre-deployed) to the closed condition (post-deployed) upon insertion. This allows for much less of the annulus fibrosis to be removed. It is important to preserve as much of the annulus fibrosis as possible because it keeps the cage in compression and allows for the bone packing material to be contained. This further ensures stability during fusion and helps optimize the final fusion of the two vertebrae. Annulus fibrosis preservation over existing cage designs is shown schematically in Fig. 9. As can be seen from the figure, the BAK-like and COUGAR®-like cages require large incisions and possible removal of multiple boney stabilizing structures. These short comings are overcome with the prototype cage.

3. Modeling

Prior to manufacture of a prototype, the torsional behavior of SMAs was numerically implemented.. A model was developed to capture the torsional response of SMAs. For thin wires and thin walled tubes, the model can be reduced in complexity to a one dimensional model. As a wire is torqued, the transformation front develops in the same manner as the classic SMA hysteresis. The visualization of the transformation for a thick wire is shown schematically in Fig. 10.

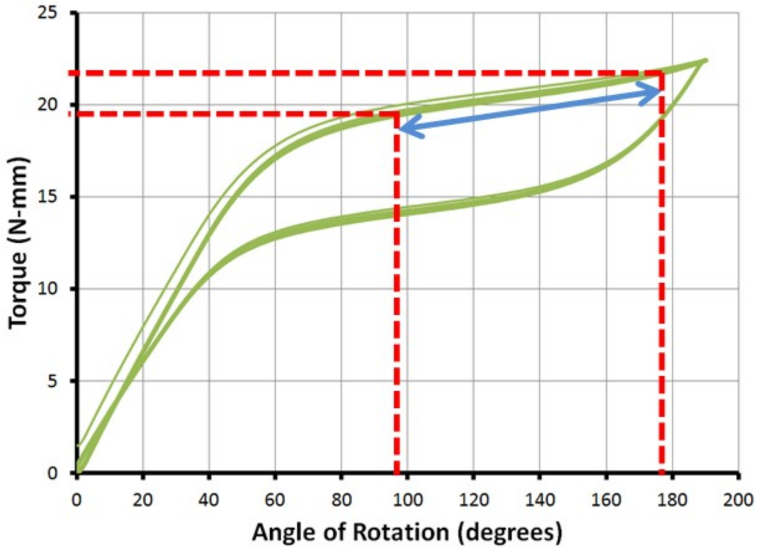

Fig. 6 Torque angle profile for the designed wire (Chapman 2011)

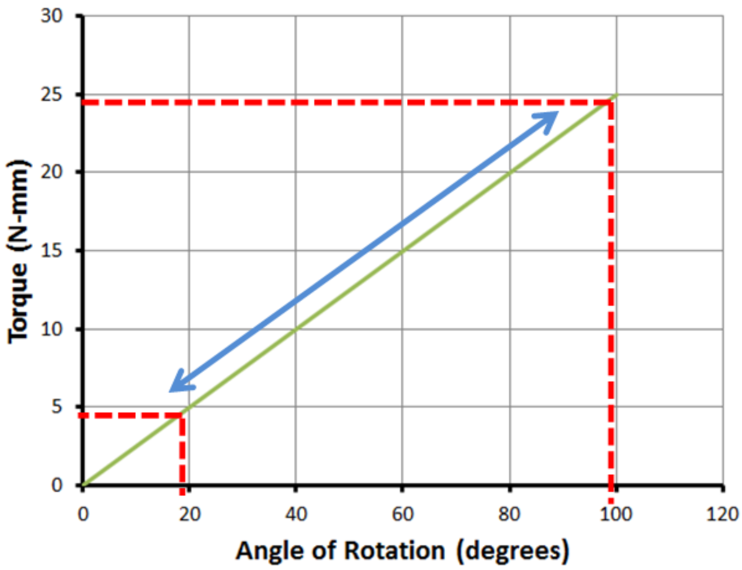

Fig. 7 Zoom of the torque angle profile for the designed wire (Chapman 2011)

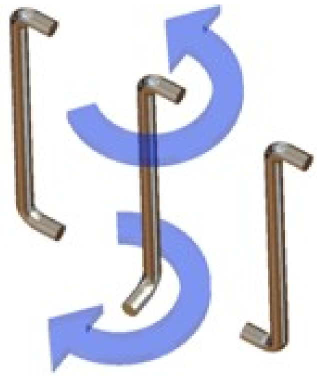

Fig. 8 Hinge concept for actuation (Chapman 2011)

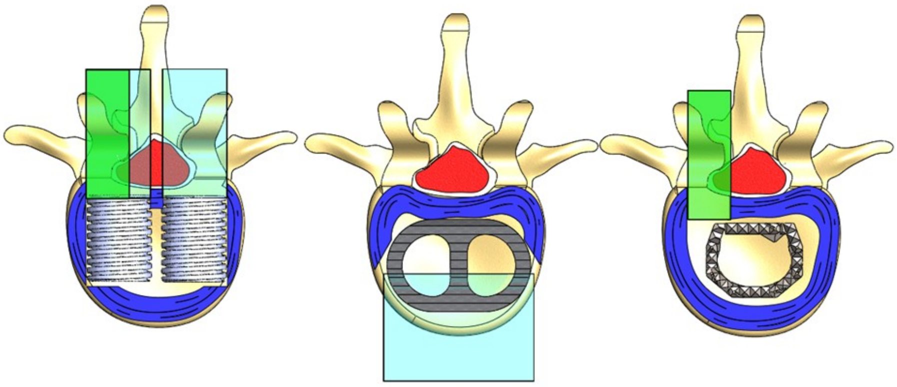

Fig. 9 Advantage of the proposed cage over existing cages; the left pane shows a BAK-like cage, the center pane shows a COUGAR®-like cage, and the right pane shows the proposed cage

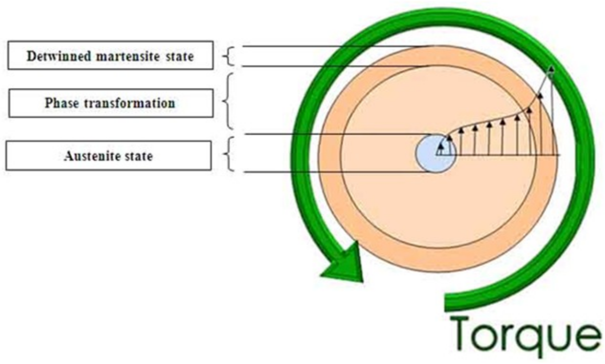

Fig. 10 Schematic showing the transformation front developing in a thick wire in torsion

However, due to the small diameter here, the shear stress is constant throughout the cross section, see Eq. (1).

$$\frac{\partial \tau}{\partial x} = 0 \tag{1}$$

where $\partial\tau$ is the change in shear stress along the change in the direction, ∂x. Eqs. (2) and (3) show how Young's modulus is changed to the shear modulus and how the angular deflection is normalized.

$$G = \frac{E}{2(1+\nu)} \tag{2}$$

$$\gamma_L = \frac{r_0 \phi}{L} \tag{3}$$

where the values of G, E, ν, γ_L, r_o, φ, and L are the Shear Modulus, Young's Modulus, Poisson ratio, maximum residual shear strain, outer radius, angle of rotation, and sample length, respectively. For thin walled tubes, the equation can be further developed into Eq. (4).

$$\tau = \frac{\tau_{applied}}{2A_m t} \tag{4}$$

where A_m is defined in Eq. (5) and t is the wall thickness.

$$A_m = \pi \left(r_0 - \frac{t}{2} \right)^2 \tag{5}$$

The shear strain can then be formulated as a function of the angle of rotation as set out in Eq. (6).

$$\gamma = \rho \frac{\partial \phi}{\partial x} \tag{6}$$

where ρ is the desired location of stress. Finally the shear stress as a function of the desired location and the applied torque can be derived as set out in Eq. (7).

$$\tau = \frac{T_{applied}}{J} \tag{7}$$

where J is the polar moment of inertia for the desired cross-section.

For a more in depth explanation of torsional modeling of SMAs, the reader is directed to (Chapman 2011, Chapman *et al*. 2011, Karbaschi 2012).

4. Experiments

To verify the torsional model, different wires were tested in torsion with two different boundary conditions, fixed and free. Different wire diameters were also tested; see Fig. 11. As can be seen in the plot, the larger wire diameter requires more torque (higher shear stress) to start transformation. Changing the boundary condition drastically affects the response of the material. It should be noted that for the 'fixed' end condition, torsion induced buckling was observed, as shown in Fig. 12. The buckling is due to the fact that nitinol exhibits the Swift effect and that flexure is energetically favorable compared to torsion (Podvratnik 2011). The results comparing the 'fixed' end condition to the 'free' end condition are shown in Fig. 13. As can be seen from Fig. 13, the buckling causes bending stress (compression-tension) to be present in the wire allowing for 2 times the generally accepted value of 8% strain. An analog to this phenomena is proportional loading. The model predicts the torsional response with fairly good agreement; see Fig. 14. The model is able to accurately capture the value for the loading and unloading plateaus, for which the hinge is designed to operate in.

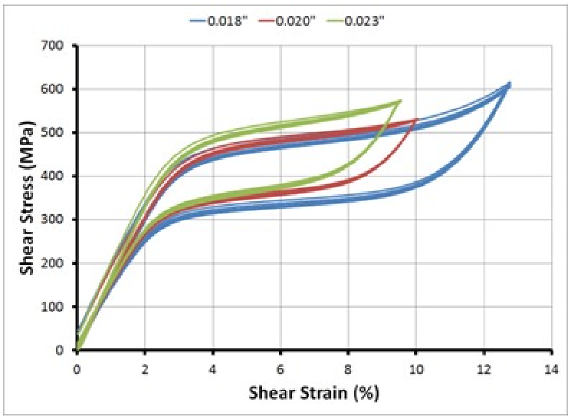

Fig. 11 Shear stress vs shear strain for the 'free' end condition (Chapman 2011)

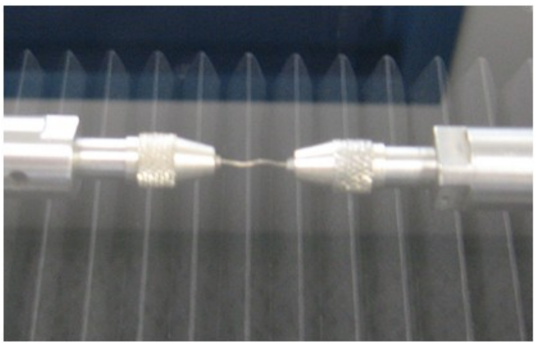

Fig. 12 Torsion induced buckling for the 'fixed' end condition (Chapman 2011)

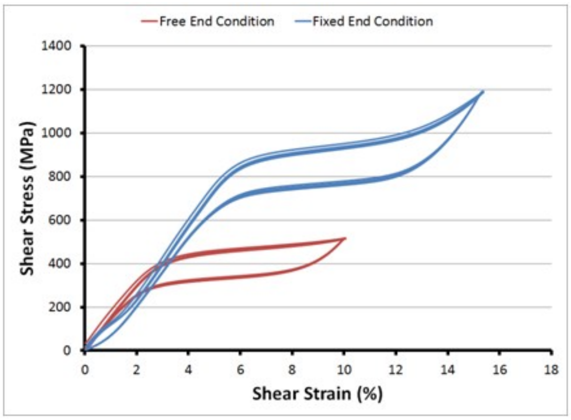

Fig. 13 Shear stress vs shear strain comparing the ‘fixed’ and ‘free’ end conditions (Chapman 2011)

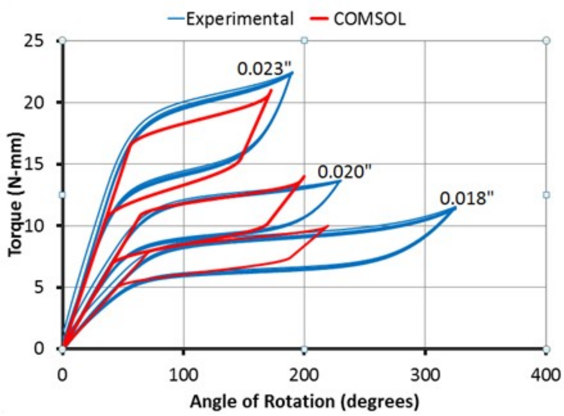

Fig. 14 Shear stress vs shear strain comparison between the experimental results and the proposed model predictions (Chapman 2011)

This model used to design the wire diameter needed for cage actuation. The plateau stress was targeted in the design due to its constant form over a large range of angular deformation. With the design established, a prototype was manufactured.

To verify the safety of the cage, experimental testing on the prototype cage was conducted. The experiments included compression testing, 45◦ (compression-shear), and torsional testing. These tests align with the static procedures set out in ASTM F2077-03 (AST). A CAD drawing showing the different testing methods is shown in Figs. 15(a)-(c). The tests were carried out on an MTS bionix 858 with a 25 kN load cell.

None of the tests resulted in cage failure. For the compression test (Fig. 15(a)), the testing conditions were a load rate of δ = 5 mm/min and a maximum loading of F_{comp} = 20 000 N. The initial stiffness of the cage in compression was 18 154 N/mm. It should be noted that the initial stiffness is defined by the 2% offset line, as per the standard. The results are shown graphically in Fig. 16.

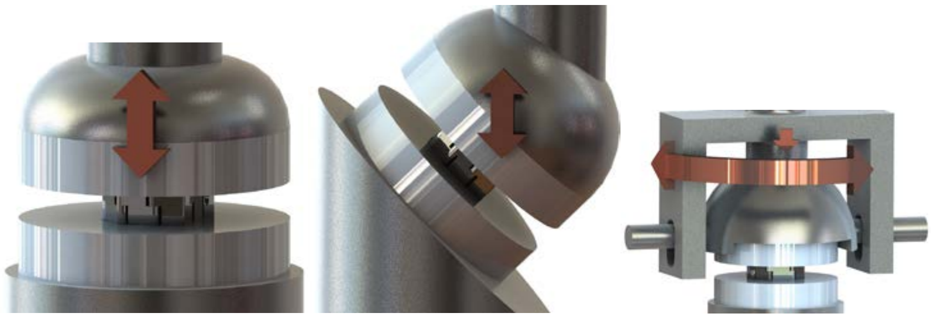

(a) Compression (b) 45°, compression-shear (c) Torsion

Fig. 15 Different ASTM testing methods for spinal fusion devices

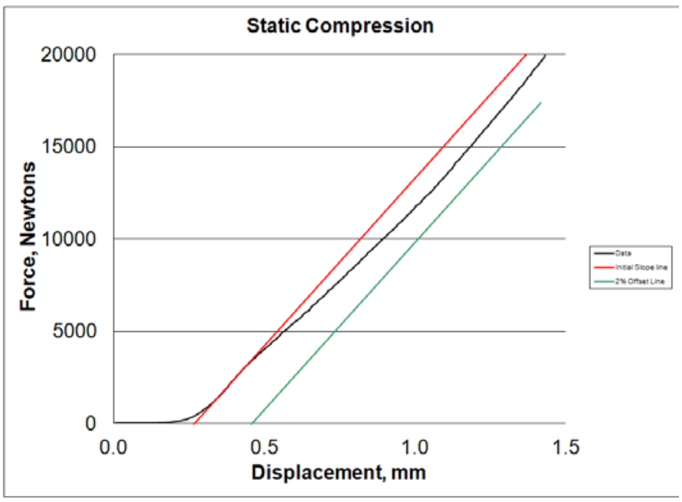

Fig. 16 Results of the test shown in Fig. 15(a)

For the compression-shear test (Fig. 15(b)), the testing conditions were a load rate of δ = 5mm/min and a maximum loading of F_{comp} = 5 000N. The initial stiffness of the cage in compression was 7 180 N/mm. The results are shown graphically in Fig. 17.

For the torsion test (Fig. 15©), the testing conditions were a load rate of δ = 5degree/min and a maximum loading of Fcomp = 15 000 N·mm. The initial stiffness of the cage in compression was 1 921 N·mm/degree. The results are shown graphically in Fig. 18.

5. Conclusions

The numerical and experimental results here show the efficacy and safety of the implant. The cage design is novel in its self-closing architecture. The model was developed based on one dimensional torsion and verified experimentally. Additionally, the difference in the boundary conditions was pointed out, showing that torsion induced buckling can lead to drastically higher recoverable strains. The model was then used to select a wire diameter for the cage to be self-closing. The prototype was then tested per an ASTM specification without observed failure. The safety and efficacy of the prototype cage has been established.

It has been shown that the spinal fusion device has the potential to survive the torturous loading conditions within the body.

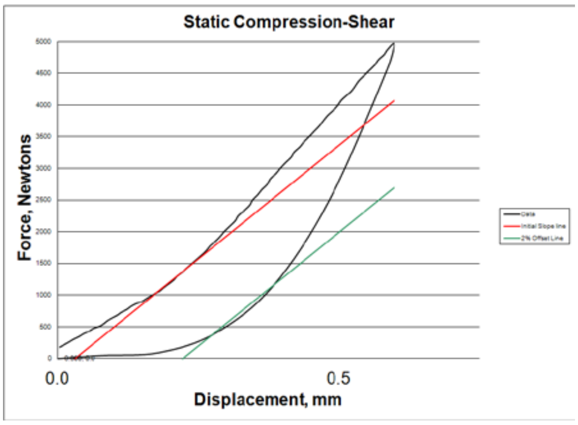

Fig.17 Results of the test shown in Fig. 15(b)

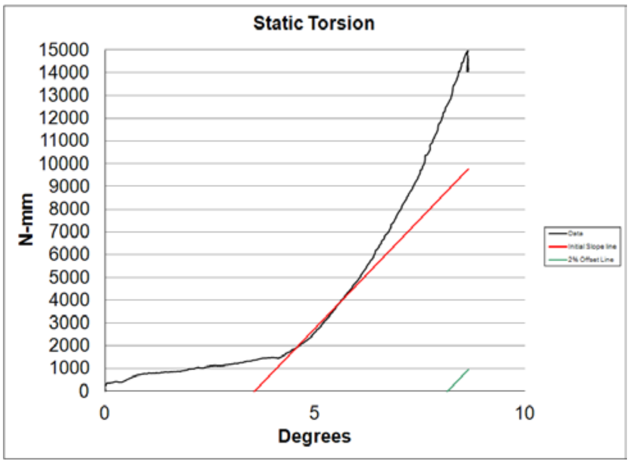

Fig. 18 Results of the test shown in Fig. 15(c)

6. Acknowledgments

Fort Wayne Metals collaborated with the authors in conducting experiments. The authors also would like to acknowledge financial support of NSF through grant CBET-0731087 as well as Ohio

Department of Development through grant WP 10-010 (Nitinol Commercialization Accelerator).

References

Assad, M., Chernyshov, A.V., Jarzem, P., Leroux, M.A., Coillard, C., Charette, S. and Rivard, C.H. (2003), "Porous titanium-nickel for intervertebral fusion in a sheep model: Part 2. surface analysis and nickel release assessment", *J. Biomed. Mater. Res. B*, **64**(2)121-129.

Bigos, S.J., Bowyer, O.R., Braen, G.R., Brown, K., Deyo, R., Haldeman, S. and Hart, J.L. (1994), *Acute low back problems in adults*, Technical report, U.S. Department of Health and Human Services. HCPR Publication No. 95-0642. Rockville, MD: Agency for Health Care Policy and Research, Public Health Service.

Boden, S.D., Moskovitz, P.A., Morone, M.A. and Toribitake, Y. (1996), Video-assisted lateral intertransverse process arthrodesis: Validation of a new minimally invasive lumbar spinal fusion technique in the rabbit and nonhuman primate (rhesus) models. Spine, 21:2689–2697. ISSN: 0362-2436.

Brennan, J. and Lauryssen, C. (2000), *Current indications for posterior lumbar interbody fuisions*, Technical report, Seminars in Neurosurgery.

Brook, G. (1983), *Applications of titanium-nickel shape memory alloys*, Materials and Design, 4.

Burkus, J. (2003), *Advances and current techniques for lumbar interbody fusion*, Operative Techniques in Orthopaedics, 13.

Chapman, C. (2011), *Design of an expandable intervertebral cage utilizing shape memory alloys*, Master's thesis, University of Toledo.

Chapman, C., Eshghinejad, A. and Elahinia, M. (2011), "Torsional behavior of niti wires and tubes: modeling and experimentation", *J. Intell. Mater. Syst. Struct*., **22**(11), 1239-1248.

Cragg, A., Lund, G., Salomonowitz, E., Rysavy, J., Castaneda, F., Castaneda-Zuniga, W. and Amplatz, K. (1983), *A new percutaneous vena cava filter*, American Roentgen Ray Society.

Duerig, T., Pelton, A. and Stockel, D. (1999), "An overview of nitinol medical applications", *Mater. Sci. Eng*., **273-275**, 149-160.

Icardi, U. and Ferrero, L. (2009), "Preliminary study of an adaptive wing with shape memory alloy torsion actuators", *Mater. Design*, **30**(10), 4200-4210.

Jacob, J.D., Simpson, A. and Smith, S. (2005), *Design and flight testing of inflatable wings with wing warping*, Technical report, University of Kentucky, Lexington, KY. Society of Automotive Engineers, Inc.

Kapanen, A., RyhaKnen, J., Danilov, A. and Tuukkanen, J. (2001), "Effect of nickel-titanium shape memory metal alloy on bone formation", *Biomaterials*, **22**(18), 2475-2480.

Karbaschi, Z. (2012), *Torsional behavior of nitinol: Modeling and experimental evaluation*, Master's thesis, University of Toledo.

Kodama, T. (1989), "Study on biocompatibility of titanium alloys", *PubMed*, **56**(2), 263-288.

Lipson, S. (2004). "Spinal-fusion surgery -advances and concerns", *N. Engl. J. Med*., **350**(7), 643-644.

Mayer, H. (1999), "The alif concept", *Eu. Spine. J.*, **9**,S35–43.

Ozgur, B. (2006), "Extreme lateral interbody fusion (xlif): a novel surgical technique for anterior lumbar interbody fusion", *Spine J*., **6**, 435-443.

Podvratnik, M. (2011). *Torsional instability of elastic rods*, University of Ljubljana.

Regan, J.J., Yuan, H. and McAfee, P.C. (1999), "Laparoscopic fusion of the lumbar spine: minimally invasive spine surgery: a prospective multicenter study evaluating open and laparoscopic lumbar fusion", *Spine J*., **24**,402-411.

Rhalmi, S., Charette, S., Assad, M., Coillard, C. and Rivard, C.H. (2007), "The spinal cord dura mater reaction to nitinol and titanium alloy particles: a 1-year study in rabbits", *Eur Spine J*., **16**, 1064-1072.

Russell, S.M. (2009), "Design considerations for nitinol bone staples", *J. Mater. Eng. Perform*., **18**(5-6), 831-835.

Ryhanen, J., Kallioinen, M., Tuukkanen, J., Junila, J., Niemela, E., Sandvik, P. and Serlo, W. (1998), "In

vivo biocompatibility evaluation of nickel-titanium shape memory metal alloy: muscle and perineural tissue responses and encapsule membrane thickness", *J. Biomed. Mater. Res*., **41**(3), 481-488.
Stoeckel, D. (2002), "Nitinol medical devices and implants", *Minm. Invasiv Ther*., **9**(2),81-88.
Test Methods For Intervertebral Body Fusion Devices, ASTM. Designation: F 2077 -03.
Walia, H., Brantley, W.A. and Gerstein, H. (1988), "An initial investigation of the bending and torsional properties of nitinol root canal files", *J. Endodont*., **14**(7), 346-351.
Wever, D., Veldhuizen, A., Sanders, M., Schakenraad, J., and van Horn, J. (1997), "Cytotoxic, allergic and genotoxic activity of a nickel-titanium alloy", *Biomaterials*, **18,**1115-1120.
Xiong, K., Tao, B. and Jin, J. (2000), *Theoretical and experimental study on shape memory alloy torsion actuator*, Technical report, ICAS 2000 CONGRESS.

CB